

Improvement of a ^3He Circulation Compressor for a Closed Cycle Dilution Refrigerator for Space

A. Nagata¹, H. Sugita², K. Shinozaki², Y. Sato²

¹University of Tsukuba, Tsukuba, Ibaraki, Japan

²Japan Aerospace Exploration Agency (JAXA), Tsukuba, Ibaraki, Japan

ABSTRACT

In astronomical observation, to achieve superior sensitivity and energy resolution, it is necessary to cool down the detector to extremely low temperature (100 mK or less) and to reduce thermal fluctuation noise emitted from the detector itself. The purpose of this research is to improve the performance of a closed-cycle dilution refrigerator for space, which is developed with the aim of cooling below 50 mK. A low suction pressure (0.4 kPa or less) with a sufficient ^3He flow rate (50 $\mu\text{mol/s}$ or more) are desired for ^3He circulator to achieve a cooling power of 1 μW at 50 mK. However, the circulator that enables low suction pressure with a high flow rate has a high technical difficulty, and it is challenging to develop. This paper describes the factors which limit the performance of the circulator and evaluate those influences by numerical analysis and compare it with experimental results. In particular, the flow path conductance performance of suction and exhaust valves, which are suggested to affect the performance of the circulator significantly, were evaluated by analysis and experiment, and the design to improve the performance of the valve was also shown.

INTRODUCTION

A low temperature detector is required for superior sensitive astronomical observation mission. To reduce thermal fluctuation noise emitted from the detector, 100 mK or lower temperature are required for high sensitivity observation satellites such as the infrared astronomical observation satellite SPICA^{1,2,3} and the X-ray observation satellite Athena^{4,5}. Currently, there are two major cooling technologies which can achieve temperatures below 100 mK. One is an adiabatic demagnetization refrigerator (ADR), and the other is a dilution refrigerator. The adiabatic demagnetization refrigerator is mechanically simple comparing the closed-cycle dilution refrigerator, and it has number of space demonstrations as a conventional cooling method^{6,7}. However, large magnetic field variance generated by the refrigerator impacts the electrical systems and the shield design of detector. A continuous ADR⁸ is still in the development phase and also has a large variance of magnetic field, and a non-negligible time for the recycling phase is also needed. On the other hand, the dilution refrigerator generates no magnetic field, and it can operate continuously. A closed-cycle dilution refrigerator can cool down to 50 mK with a comparable cooling power as an adiabatic demagnetization refrigerator but a 100% duty cycle in principle. Therefore, this is expected to be a new generation space refrigerator. The closed-cycle dilution refrigerator is an advanced design based on the open-cycle dilution refrigerator mounted in the Planck satellite⁹ and has the possibility to provide a breakthrough in space refrigerator by making the lifetime 2 times longer (> 5 years) with

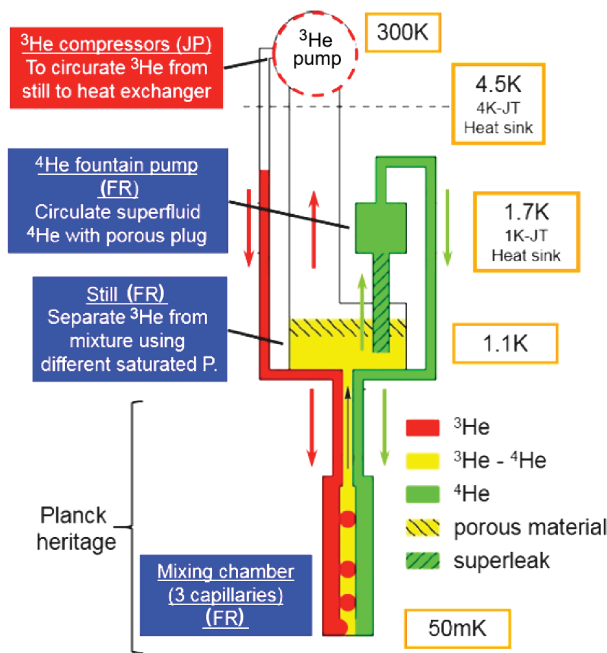


Figure 1. The schematic drawing of the closed-cycle dilution refrigerator.¹²

10 times more cooling power than the open-cycle dilution refrigerator^{10,11}. Currently, the closed-cycle dilution refrigerator was developed with a target cooling power of $1\mu\text{W}$ at 50mK and target life-time of more than 5 years. The previous experimental results show that it has achieved cooling to below 70mK under gravity, but lower inlet pressure and higher flow rate of ^3He is desired to realize higher cooling power at 50mK¹². The purpose of this research is decreasing inlet pressure with higher flow rate of ^3He to improve the cooling power of the closed-cycle dilution refrigerator.

CONFIGURATION OF THE DILUTION REFRIGERATOR FOR SPACE

The closed-cycle dilution refrigerator brings low temperature by using an endothermic reaction from diffusion with a movement of ^3He from $^3\text{He-C}$ (condense) phase to $^3\text{He-D}$ (dilute) phase. Shown in Fig. 1 are the helium circulation lines of the closed-cycle dilution refrigerator¹². That was

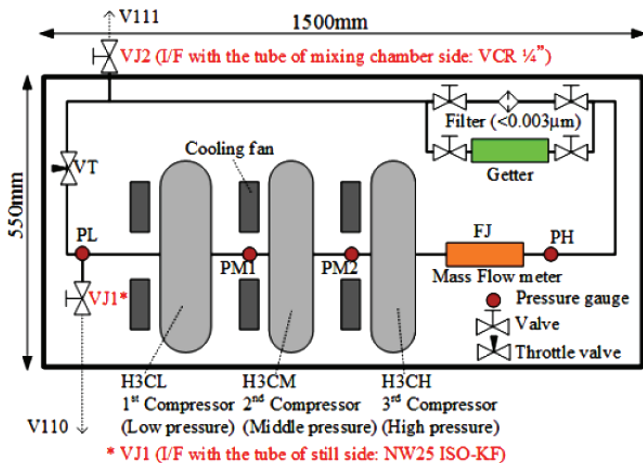


Figure 2. The schematic drawing of the ^3He circulator using 3 units of compressors.

Table 1. The objective performance

Target	³ He circulator	Compressor for 1K-JT
³ He flow rate	≥50 μg/sec	744 μg/sec
Inlet pressure	≤0.4 kPa	8 kPa
Outlet pressure	≥12 kPa	70 kPa
Drive power	<40 W	<75 W

designed to operate under a microgravity environment. On the ground, the interface between ³He-D phase and ³He-C phase naturally forms due to gravity (due to density difference). On the other hand, under microgravity, the interface is formed using capillary force.¹³

The ³He circulator is constructed from three compressors, H3CL (low pressure), H3CM (middle pressure) and H3CH (high pressure) as shown in Fig. 2. Each compressor compresses the (shown in Fig. 3) ³He working gas with two facing pistons, to straighten the gas flow through the inlet and outlet valves.

Currently, ³He the circulator is under development based on the compressor developed for a 1 K class Joule Thomson Refrigerator¹⁴ (1 K-JT refrigerator) as shown in Table 1, and a suction pressure lower than 0.4 kPa is required. Though the inlet pressure of 8 kPa for the 1K-JT is assumed to be the lowest pressure provided by a space qualified compressor, it is still challenging that the inlet pressure design must be improved to achieve greater than 1/10 lower target inlet pressure (8 kPa → 0.4 kPa)¹².

To realize the suction pressure of 0.4 kPa, it is necessary to appropriately evaluate the leakage and pressure loss from the valves and the pistons which have been thought not to be dominant previously. Since there are few studies in the past for a piston compressor with the low-pressure requirement shown in Table 1, the research is highly valued for understanding it.

LIMITING FACTORS FOR THE PERFORMANCE OF ³HE COMPRESSOR

Shown in Fig. 4 are measured inlet/outlet pressures as a function of flow rate from a previous performance test. It is necessary to increase the flow rate while keeping the suction pressure as low as 0.4 kPa or less for the ³He circulator to obtain the required performance shown in Table 1. Major design parameters that are considered to limit the performance of ³He circulator are listed below, and each description is shown in Fig. 5.

- 1. Leakage from the suction/exhaust valve.
- 2. Leakage from the piston clearance.
- 3. Insufficient compression ratio caused by dead volume.
- 4. Insufficient piston stroke.
- 5. Insufficient valve flow path conductance.

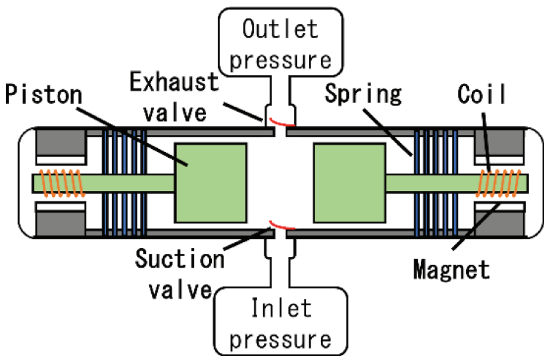


Figure 3. The schematic drawing of the ³He compressor¹²

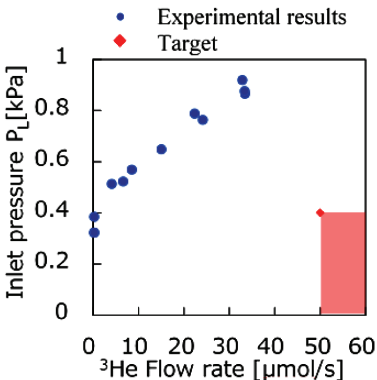


Figure 4. Relationship between flow rate and suction pressure of the ³He circulator (target and experimental results)

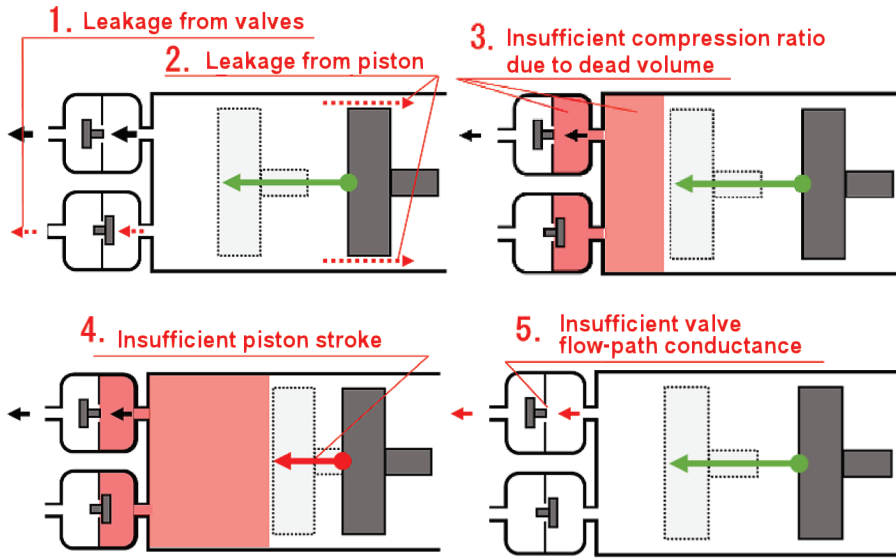


Figure 5. Schematic drawing of the model of the ^3He circulator

The influences on the circulator performance (the flow rate in the low-pressure condition) provided by each parameter were evaluated by comparing a numerical analysis with the experimental results. Fig. 6 shows the outline of the mathematical model used for analysis.

The numerical analysis results in which each parameter's effects on the compressor performance are summarized below.

1. Leakage from suction/exhaust valve

From the results of sensitivity analysis by numerical calculation, shown in Fig. 7, and the leakage measurement with the actual ^3He circulator, it suggests that this leakage reduces the flow rate by only about 5% in an ideal compressor as compared with the case of no leakage. Therefore, it is not considered to be the main factor limiting the performance of the compressor.

2. Leakage from piston clearance

From the results of sensitivity analysis by numerical calculation, shown in Fig. 8, and the leakage measurement using the actual ^3He circulator, it suggests that this leakage reduces a flow rate by only about 5% in an ideal compressor as compared with the case of no leakage. Therefore, it is not considered to be the main factor limiting the performance of the compressor.

3. Insufficient compression ratio originated from dead volume

From the results of sensitivity analysis by numerical calculation, shown in Fig. 9, and the leakage measurement using the actual ^3He circulator, it is considered that this factor reduces a flow rate by only about 7% in an ideal compressor as compared with the case of no leakage. Therefore, it is not considered to be the main factor limiting the performance of the compressor.

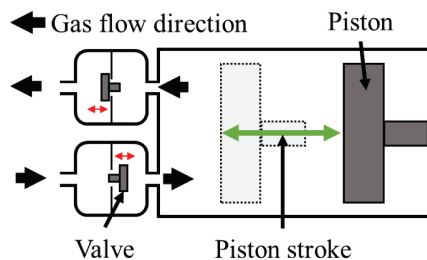


Figure 6. Description of factors that are considered to limit the performance of ^3He circulator

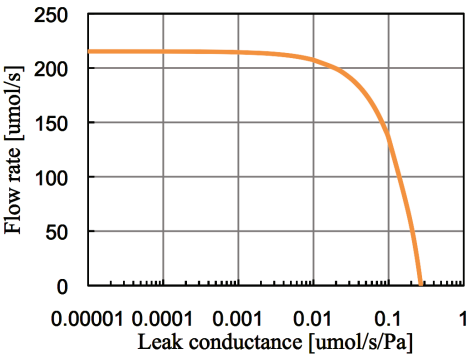


Figure 7. The relationship between the leak conductance of suction/exhaust valve and the flow rate of the ³He circulator.

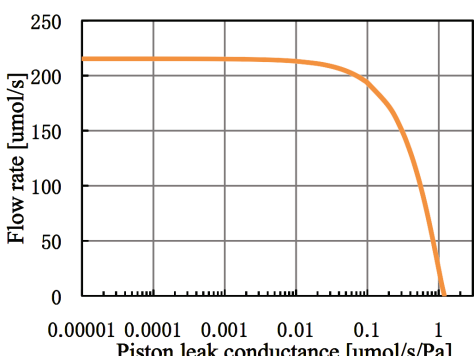


Figure 8. The relationship between the leak conductance of piston clearance and the flow rate of the ³He circulator.

4. Insufficient piston stroke

This factor decreases the flow rate with a sensitivity of 74.06 [$\mu\text{mol} / \text{s} / \text{mm}$] against change with the piston stroke, shown in Fig. 10. The current design stroke is $\pm 5 \text{ mm}$ and the flow rate decreases about 15% (33 [$\mu\text{mol} / \text{sec}$]) when the stroke is reduced 5%. This parameter influences the compression performance effectively and piston stroke should be strictly managed.

5. Insufficient valve flow path conductance

The relationship between a flow rate of the compressor and valve flow path conductance was evaluated by numerical analysis, shown in Fig. 11-12. From this result, the requirement of a

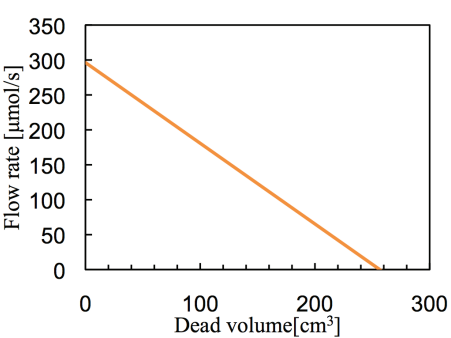


Figure 9. The relationship between the dead volume and the flow rate of the ³He circulator.

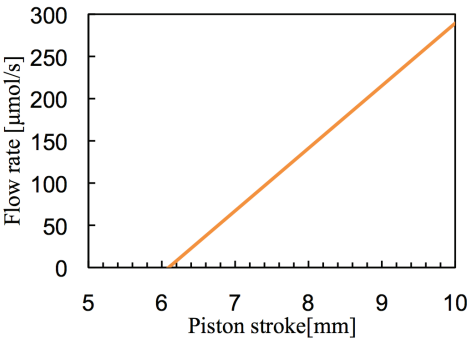


Figure 10. The relationship between the piston stroke and the flow rate of the ³He circulator.

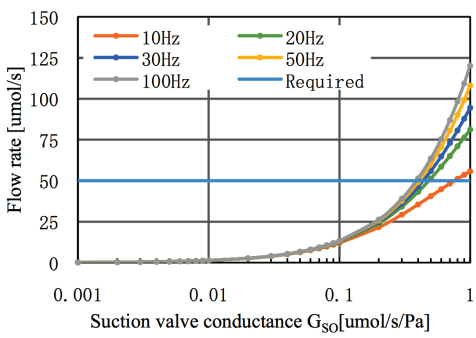


Figure 11. The relationship between the flow path conductance of suction valve and the flow rate of the ³He circulator.

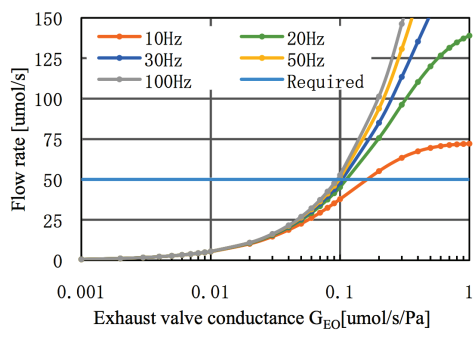


Figure 12. The relationship between the flow path conductance of exhaust valve and the flow rate of the ³He circulator.

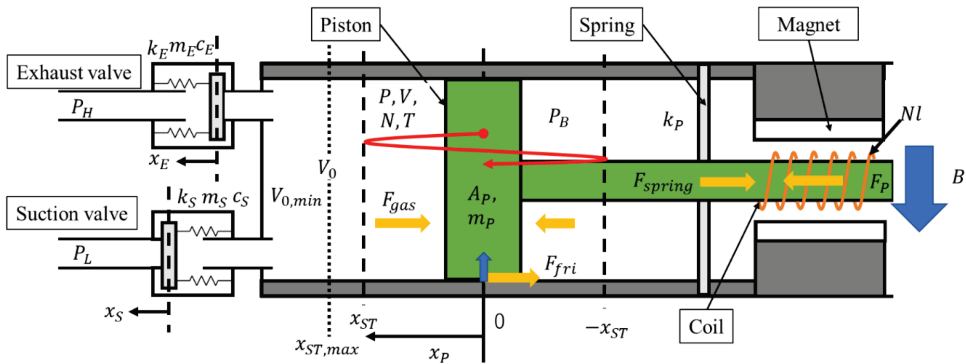


Figure 13. Numerical analysis model of the ^3He compressor

minimum necessary flow path conductance was found for the discharge valve and suction valve for satisfying the target flow rate. Currently, valve flow path conductance has not been measured, thus it is an unknown value, and insufficient flow path conductance is assumed to be a significant factor limiting the performance of the compressor.

These results mentioned above found the possibilities that insufficient piston stroke and insufficient valve flow path conductance have a relatively significant effect on the compression performance. In the next section, modeling of the valve behavior and the valve flow path conductance was performed to evaluate the effect of the valve flow path conductance on the circulator flow rate.

MODELING OF VALVE BEHAVIOR AND FLOW PATH CONDUCTANCE

In this section, the valve behavior and valve flow conductance were modeled from the viewpoint of mechanical and molecular flow dynamics. Through the comparison of the previous experimental results and the analysis results, the validity of the numerical model was confirmed.

Valve Behavior

The behavior of the valves in the compressor were modeled. Shown in Fig. 13 is the outline of the mechanical model of the ^3He circulator.

Piston motion in the linear compressor can be written as follow:

$$m_P \ddot{x}_P = F_{spring} + F_{fri} + F_{gas} + F_P \quad (1)$$

For simplicity, the piston position is expressed as a sinusoidal oscillation and the pressure inside the compression chamber is assumed as an ideal gas state relationships.

Reed valves are used in the ^3He compressor. These valves are essentially cantilevered beams which are passively driven by differential pressure across them. This model focus on the displacement of the tip of the valve and the movement of the valve is expressed and analyzed as a spring-mass system. Shown in Fig. 14 is the valve modeled as a beam. The area where the differential pressure

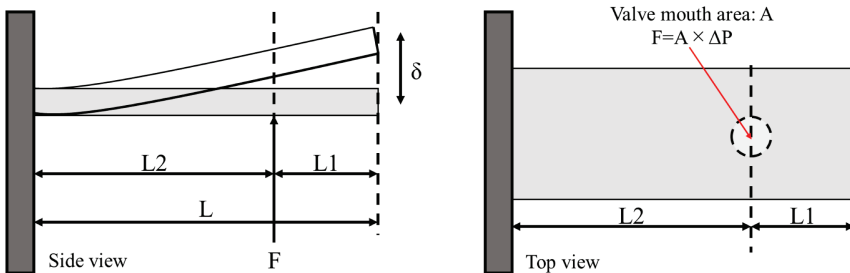


Figure 14. The mechanical model of the valve using beam theory

acts on the valve may be varied depending on the opening width of that, but in this research, the area is assumed the cross-section of the valve hole for simplicity.

The spring constant k for tip displacement (δ) is calculated in the following equations:

$$\delta = \frac{FL_2^2(3L_1 + 2L_2)}{6EI} \quad (2)$$

$$k = \frac{F}{\delta} = \frac{6EI}{L_2^2(3L_1 + 2L_2)} \quad (3)$$

Also, the effective mass (m_{beam}) is defined so that the natural frequency of the valve is equal between beam model and spring-mass model.

$$\begin{aligned} m_{beam} &= k \times \frac{\rho AL^4}{1.875^4 \times EI} \\ &= \frac{6\rho AL^4}{1.875^4 \times L_2^2(3L_1 + 2L_2)} \end{aligned} \quad (4)$$

Flow Path Conductance

From the equation (2), the maximum value of the valve opening width (D_{max}) under the maximum differential pressure condition is calculated using the mechanical characteristics. The maximum differential pressures for exhaust and suction valve are calculated as:

$$P_{diff_ex} = P_L \times \frac{V_{max}}{V_{min}} - P_H \quad (5)$$

$$P_{diff_su} = P_L - P_H \times \frac{V_{min}}{V_{max}}. \quad (6)$$

The results of the calculation are shown in Table 2. From the calculation results, it is found that the maximum opening width of the suction valve is 1.17 μm and that of the discharge valve is 54.8 μm . Next, the type of flow is investigated using the calculated valve opening width. The form of flow is estimated by the Knudsen number (K) calculated from the ratio of the mean free path length (λ) for He and the opening width of the valve.

$$\lambda = \frac{kT}{\sqrt{2}\pi d^2 P} \quad (7)$$

$$K < \lambda/D_{max} \quad (8)$$

where the form of flow is estimated as:

$$K \ll 1 : \text{viscous flow} \quad (9)$$

$$K \geq 1 : \text{molecular flow.} \quad (10)$$

Table 2. Valve opening width and Form of flow

	Suction valve	Exhaust valve
Maximum differential pressure [Pa]	303	5029
Maximum opening width [m]	1.17×10^{-6}	5.48×10^{-5}
Mean flow path length [m]	4.90×10^{-5}	1.23×10^{-5}
Form of flow	molecular flow	molecular flow or transition flow

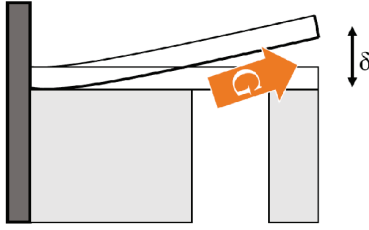


Figure 15. Outline of the flow path conductance model of the valve

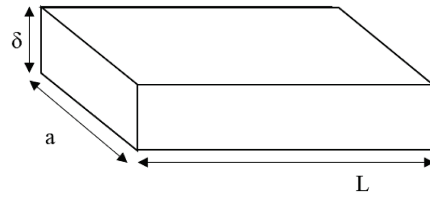


Figure 16. Flow path model formed at valve opening

From the estimation, the type of flow for the suction valve is estimated as molecular flow and the form for the exhaust valve is estimated as molecular or transition flow.

The valve flow path conductance was modeled assuming molecular flow. Shown in Fig. 15 and Fig. 16 are the models for the flow path formed during the valve opening.

The flow path conductance of molecular flow can be derived. In general, the flow conductance of molecular flow through a circular pipe can be expressed as follow:

$$G = \frac{2\pi a^3 \bar{v}}{3L} \quad (11)$$

here a and L are the radius and the length of pipe, \bar{v} is the average speed of gas molecules, and it is a constant when the temperature is constant. By rearranging equation (11), the following equation can be obtained.

$$G = \frac{4(\pi a^2)^2 \bar{v}}{3(2\pi)L} = \frac{4A^2 \bar{v}}{3BL} \quad (12)$$

here A is the cross-sectional area of the flow path, B is the circumferential length. The model of Fig. 16 is applied to equation (12), then substituting $A = a \times \delta$, $B = 2(a + \delta)$ to this equation. Thus, equation (12) is rearranged as follow:

$$G = \frac{4a^2 \delta^2 \bar{v}}{6(a + \delta)L} \quad (13)$$

here, from $\delta \ll a$, equation (13) can be rearranged as:

$$G \approx \frac{4a^2 \delta^2 \bar{v}}{6aL} = \frac{2a \delta^2 \bar{v}}{3L} \propto \delta^2 \quad (14)$$

From equation (14), the flow path conductance G is proportional to the square of the valve opening width δ .

Comparison of Analysis and Experimental Results

The flow rate of the compressor was predicted by analysis using valve flow conductance model. Boundary conditions were set the same as that of previous experiments. The finite difference method was used for the analysis.

The comparison of experimental results with analysis results is shown in Table 3 and Fig. 17. The model results were in good agreement with the experimental results at each boundary condition and all results were within a difference of 2.6 $\mu\text{mol/sec}$ between analysis and experimental results, as shown Table 3 and Fig. 17. These differences are due to the measurement error in the experimental results, and the influences, as discussed in previous chapter, of leakage and insufficient piston stroke. Since the correlation coefficient between experimental results and analysis results shows a strong correlation of about 0.99, this analysis model has adequate accuracy to predict experimental results. Therefore, insufficient flow path conductance due to insufficient valve opening width is assumed to be a major factor limiting the performance of the circulator.

Table 3. The comparison of experimental and analysis results

Boundary condition No.	P_L [Pa]	P_H [Pa]	Experimental results Flow rate [$\mu\text{mol/s}$]	Analysis results Flow rate [$\mu\text{mol/s}$]
1	327	1340	0	0.96
2	327	2000	0	0.55
3	388	1620	0	1.42
4	517	1720	3.87	4.31
5	527	1620	6.2	4.93
6	573	1580	8.18	6.96
7	652	1390	14.7	12.3
8	768	1410	24.0	22.0
9	792	1820	21.9	21.0
10	869	1450	33.1	33.2
11	880	1450	33.2	34.6
12	923	1910	32.7	35.3

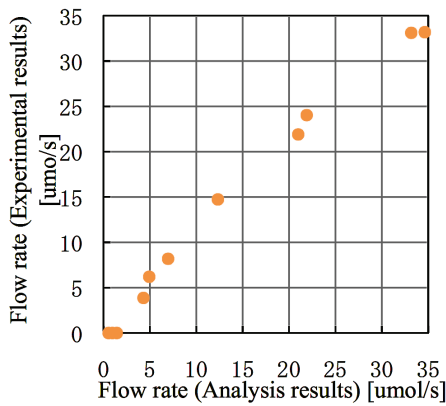


Figure 17. The comparison of analysis results and experimental results

Method to Improve the Performance of the Circulating Compressor

In this section, the possibility of improving the performance of the compressor by changing the design parameters of the valve using the established analysis model is investigated. Table 4 shows an example of the analysis result for the flow rate performance by changing valve parameters. Valve parameters used for the analysis are summarized in Table 5. In the valve design values in Table 4, the current design value is set to 1, and the ration for that is written as the value after the design change. The variables in Table 5 represent the parameters of the beam model of Fig. 14.

From the analysis using values shown in Table 5, a significant increase in flow rate can be expected by changing the design value of the length, the position of the hole and width of the valve. Increased flow rate can be expected by decreasing the spring constant of the valve.

Table 4. The examples of flow rate prediction after valve design change

Boundary condition No.	Experimental results Flow rate [$\mu\text{mol/s}$]	Optimized design (analysis) Flow rate [$\mu\text{mol/s}$]
1	0	49.2
4	3.87	74.3
5	6.2	155.0

Table 5. The ratio of the valve design value used for analysis of the improvement method against the original valve design value. (the original values are set to 1)

	Suction valve	Exhaust valve
Valve length: L	1.875	1.263
Distance to valve hole: L_2	2.0	1.357
Valve width: W	1	0.22

CONCLUSION

In this study, improvement of ^3He compressor was discussed for the closed-cycle dilution refrigerator for space. Currently, the ^3He circulation compressor needs a design update to obtain the target specification of an inlet pressure 0.4 kPa or less and with a higher flow rate 50 $\mu\text{mol/sec}$. In this study, the main design parameters that were considered to limit the performance of ^3He circulator were discussed and the influences of each factor for the flow rate was evaluated by numerical analysis.

As results of this study, the following was found out.

1. Leakage from suction/exhaust valve and piston clearance, and the factor of insufficient compression ratio originated from dead volume, are not the main cause of limiting the performance of the compressor.
2. Piston stroke has a high sensitivity to the flow rate and strict management is important. Observation for the piston stroke and appropriate control are necessary.
3. The valve flow path conductance is assumed to be a very sensitive parameter with respect to the total flow rate and is the main factor causing the current flow rate reduction.
4. Modeling by considering the flow around the valve as a molecular flow shows a very good agreement with the experimental results. From the above results, the insufficient valve flow path conductance originated from the insufficient opening width is assumed to be the main cause of the reduction of the flow rate.
5. Increasing the flow rate of the compressor can be expected by changing the design of the valve to decrease the spring constant, and improvement of the compressor performance is expected.

REFERENCES

1. Nakagawa, T., et al., "The next-generation infrared astronomy mission SPICA under the new framework," *Space Telescopes and Instrumentation 2014: Optical, Infrared, and Millimeter Wave*, Vol. 9143 (2014).
2. K. Shinozaki, et al., "Thermal study of payload module for the next-generation infrared space telescope SPICA in risk mitigation phase," *Cryogenics*, Vol. 64 (2014), pp. 228–234.
3. T.Nakagawa et al., "The Next-Generation Infrared Space Mission SPICA: Project Updates," *Publications of The Korean Astronomical Society*, Volume 32, Issue 1,(2017), pp.331-335.
4. Ravera, L., et al., "The X-ray Integral Field Unit (X-IFU) for Athena," *Space Telescopes and Instrumentation 2014: Optical, Infrared, and Millimeter Wave*, Vol. 9144 (2014).
5. D.Barret et al., "The Athena X-ray Integral Field Unit (X-IFU)," *Space Telescopes and Instrumentation*, (2018).
6. R. L. Kelley et al., "The Suzaku High Resolution X-Ray Spectrometer," *Publications of the Astronomical Society of Japan*, Vol. 59 (2007), pp. S77-S112.
7. Tsujimoto Masahiro, et al., "In-orbit operation of the soft x-ray spectrometer onboard the Hitomi satellite," *Journal of Astronomical Telescopes, Instruments, and Systems*, Vol. 4, no. 1, (2018).
8. Peter. Shirron., et al., "An adiabatic demagnetization refrigerator capable of continuous cooling at 10mK and below," *Nuclear Instruments and Methods in Physics Research Section A: Accelerators, Spectrometers, Detectors and Associated Equipment* 559, (2006), pp. 651–653.
9. Triqueneaux, S. et al., "Design and performance of the dilution cooler system for the Planck mission," *Cryogenics*, Vol. 46 (2006), pp.288-297.

10. Martin S, et al., "Status of the closed-cycle dilution refrigerator for space applications," *Journal of Low Temperature Physics* (2014), pp. 1069-1074.
11. G. Chaudhry, et al., "A closed-cycle dilution refrigerator for space applications," *Cryogenics*, Vol. 52 (2012), pp. 471–477.
12. K. Shinozaki, et al., "Development of Helium-3 Compressors and Integration Test of Closed-Cycle Dilution Refrigerator System," *Transactions of The Japan Society for Aeronautical and Space Sciences*, Japan 14 (2016), pp. 27-31.
13. C. Philippe, et al., "Status of the Closed-Cycle Dilution Refrigerator Development for Space Astrophysics," *Journal of Low Temperature Physics*, 176(5-6) (2014), pp. 1069-1074.
14. Y. Sato, et al., "Development of 1K-class Joule–Thomson cryocooler for next-generation astronomical mission," *Cryogenics*, Vol. 74 (2016), pp. 47–54.